Title

Improved immunofluorescence staining protocol for STED nanoscopy of *Plasmodium*-infected red blood cells

Authors

Ann-Kathrin Mehnert[a], Julien Guizetti[a *]

Affiliations

[a] Department of Infectious Diseases, Parasitology, Heidelberg University Hospital, Im Neuenheimer Feld 324, 69120 Heidelberg, Germany.

[*] Corresponding author.
Department of Infectious Diseases, Parasitology, Heidelberg University Hospital, Im Neuenheimer Feld 324, 69120 Heidelberg, Germany.
E.mail address: julien.guizetti@med.uni-heidelberg.de

Highlights

- Seeding infected red blood cells allows fixation without glutaraldehyde
- Omitting glutaraldehyde improves immunofluorescence staining
- STED nanoscopy is readily applicable to infected red blood cells

Abstract

Immunofluorescence staining is the key technique for visualizing organization of endogenous cellular structures in single cells. Labeling and imaging of blood stage *Plasmodium falciparum* has always been challenging since it is a small intracellular parasite. The gold standard for parasite immunofluorescence is fixation in suspension with addition of minute amounts of glutaraldehyde to the paraformaldehyde-based solution. While this maintains red blood cell integrity, it has been postulated that antigenicity of the parasite proteins was, if at all, only slightly reduced. Here we show the deleterious effect that even these small quantities of glutaraldehyde can have on immunofluorescence staining quality and present an alternative cell seeding protocol that allows fixation with only paraformaldehyde. The highly improved signal intensity and staining efficiency enabled us to carry out STED nanoscopy on nuclear substructures.

Keywords

Malaria; *Plasmodium falcparum*; Blood stage; Immunofluorescence; STED; Super-resolution

Over the last decade significant progress in understanding the cell biology of malaria parasites has been made [1]. Despite advances in live cell tagging technologies, immunofluorescence staining is still the best alternative to localize unaltered endogenous proteins in their native context [2]. The red blood cell (RBC) stage of the *Plasmodium falciparum* parasite is particularly challenging to stain due to multiple membranes hindering antibody penetration, the autofluorescence of the host cell, and its sensitivity to osmotic changes, causing lysis under many conditions. Tonkin *et al.* have made a great effort in determining the minimally required glutaraldehyde (GA) concentration (0.0075%) to prevent RBC lysis throughout the whole in suspension immunofluorescence staining procedure [3]. Paraformaldehyde (PFA) fixation alone is not a viable option for immunofluorescence staining in suspension because RBC lysis after or during permeabilization makes the recovery of parasites impossible. This protocol is widely used in the field and has significantly contributed to the progress around many diverse cell biological questions. However, GA fixation remains a compromise. Its deleterious effects on immune epitopes, quenching of fluorescent proteins, and increase of background fluorescence at higher concentrations are well-known. We suspected that even minute amounts of GA are still masking valuable epitopes for many of the used antibodies. Alternative fixation methods such as methanol, air drying, or saponin-lysed parasites have been used but are clearly inferior in terms of structural preservation. Also glyoxal, which has been recently highlighted as a superior fixative for many vertebrate/mammalian cell lines in terms of structural preservation and staining efficiency [4], did not work efficiently in *Plasmodium* blood stage (Suppl. Fig. 1). Another key limitation to studying parasite cell biology, and especially nuclear biology, is the parasite's comparatively small size. This limitation has been partially overcome by applying structured-illumination microscopy (SIM) during invasion studies [5]. SIM is however physically limited to a doubling of resolution [6]. More advanced super-resolution imaging technologies heavily rely on optimal sample preparation, good signal-to-noise ratio, and high signal intensities [7]. Here, we demonstrate the possibility to omit GA from the fixation protocol by combining immunofluorescence with cell seeding on imaging dishes as established by Grüring *et al.* for live cell imaging [8,9]. This resulted in a substantial improvement of labeling intensity, specificity and efficiency while maintaining structural integrity of the parasite cells. Additionally, we show that several antibodies that have previously been discarded as unsuitable for *P. falciparum* staining can actually produce satisfactory results under those conditions. This improved immunofluorescence protocol enabled us also to acquire high quality STED pictures of sub-diffraction nuclear structures, i.e. nuclear pores and hemi-spindle microtubules.

To avoid the problems with RBC lysis in suspension explored the possibility to seed the cells in concanavalin A-coated imaging dishes, as described by Grüring *et al.*, prior to fixation and staining [9]. This prevented parasite loss during fixation with 4% PFA only and allowed us to explore the effect of 0.0075% GA addition on the quality of immunofluorescence staining. Without GA we observed a change of the infected RBC (iRBC) monolayer from red-brown to clear after the permeabilization step, suggesting that the RBC cytoplasm was at least partially washed out. We found that RBCs were structurally slightly altered and became significantly more translucent in the brightfield channel (Fig. 1A) but also less autofluorescent. Host cell actin staining with phalloidin revealed a more irregular RBC membrane shape whereas the staining intensity was much increased. However, we did not observe any loss of parasite density on the slide. From a practical aspect, this staining technique achieves very consistent monolayers with high parasitemia, avoids centrifugation steps, and facilitates potential combination with live cell imaging. Using parasitophorous vacuole staining with anti-Exp1 antibodies [11], we observed that the three-dimensional structure of the parasite showed neither structural alterations nor flattening of the parasite itself or its nucleus (Fig. 1B). This is consistent with the observation that partial RBC lysis only occurs well after fixation is completed, allowing the parasite to maintain its shape. We observed, however, strongly increased Exp1 signal intensity without GA and a much higher labeling density. When the same cell was z-projected, the anti-Exp1 signal is only barely detectable in the GA-fixed samples under identical acquisition and contrast settings (Fig. 1C). This prompted us to test this improved staining protocol for several antibodies targeting different parasitic structures representing the RBC cytoplasm, the parasite outer membrane, parasite cytoplasm, the nuclear membrane and the nucleoplasm. Labeling with anti-α-tubulin (T5168, Sigma) antibodies revealed much brighter staining of nuclear microtubules under identical conditions while displaying the same protein organization (Fig. 1D). When fixed in the presence of GA, both centriolar plaques and hemi-spindle microtubules were only detectable if contrast settings for the anti-α-tubulin signal were adjusted accordingly (Fig. 1D). Anti-PfNup116 (nuclear pores, [13]) staining in contrast yielded comparable

signal intensities when fixed either with or without GA (Fig. 1E). We found that in this case primarily background binding of the respective antibody was reduced in GA-free conditions. Staining with anti-SBP1 (Maurer's clefts, [12]) antibodies, although the same localization pattern is maintained, is much more efficient without GA in all cells observed (Fig. 1F). Our results suggest that even those small quantities of GA can modify immune epitopes, causing a decline in specific antibody binding.

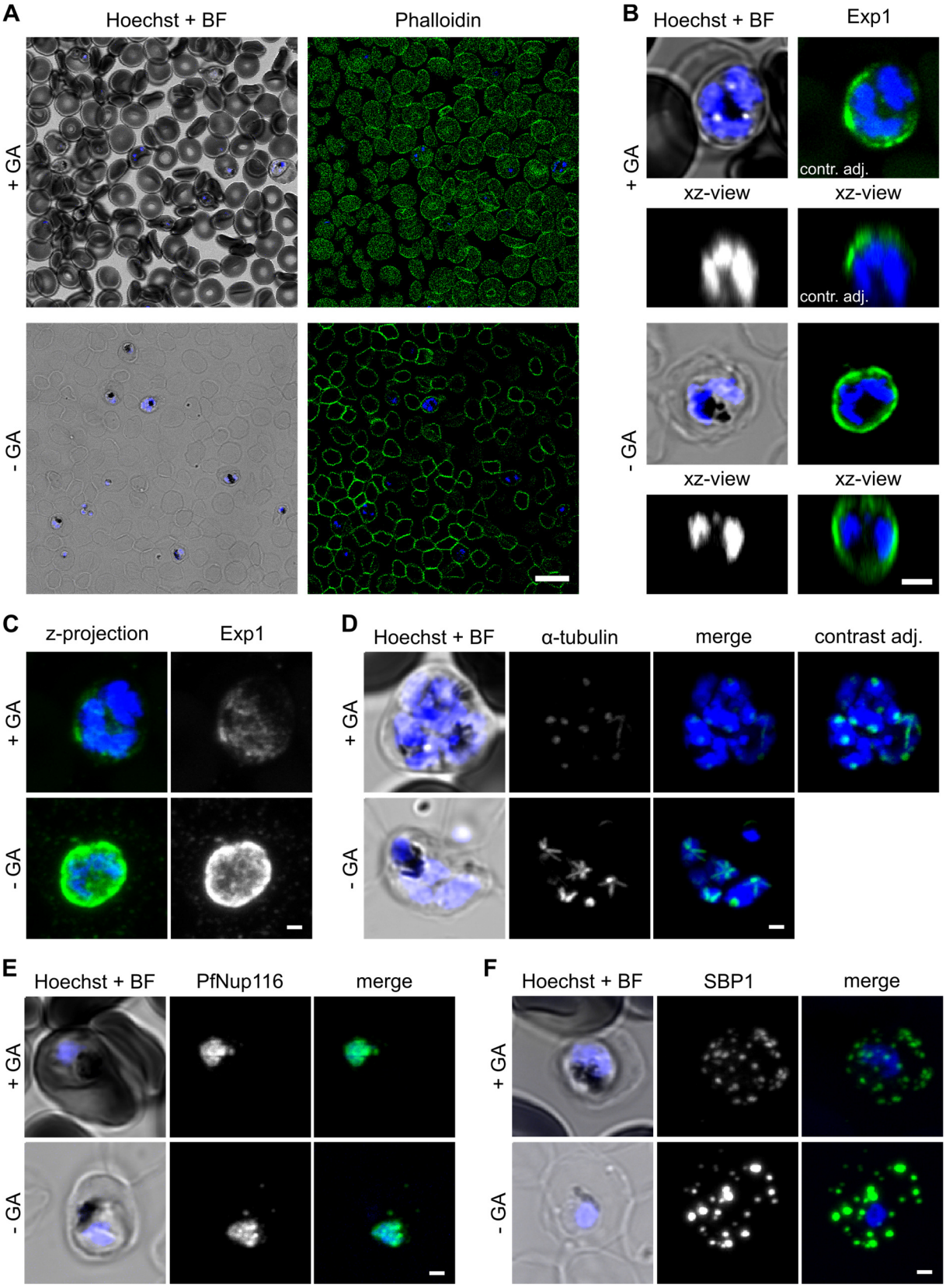

Fig. 1. Infected RBC morphology and immunofluorescence staining efficiency after fixation without GA. *(A) Confocal overview images of iRBCs stained with Phalloidin-Alexa Fluor 488 (green) and Hoechst (blue) after either fixation with (upper panel) or without addition of GA (lower panel). Scale bar, 10 µm. (B) Confocal slice images of iRBCs stained with Hoechst (blue) and labeled with anti-Exp1 antibody (green, dilution 1:500). To illustrate the three-dimensional shape of the parasite, xz-views of the same cells are shown in each panel. Contrast adjustments are different for +GA (Min: 0, Max: 30) and –GA (Min: 0, Max: 150) samples to allow visibility of the signal. Scale bar, 2 µm. (C) Maximum intensity projection of z-stacks of the same cells as in (B), labeled with anti-Exp1 antibody after either fixation with (upper panel) or without GA (lower panel). Identical contrast settings (Min: 0, Max: 150) were applied to highlight differences in signal intensities. Scale bar, 1 µm. (D)–(F) Confocal images of iRBCs, fixed either with (upper panels) or without GA addition (lower panels), stained with Hoechst (blue) and labeled with antibodies for various parasitic structures (green). These include (D) α-tubulin (microtubules, dilution 1:500). To allow comparable visibility of the anti-α-tubulin signal under identical acquisition conditions, contrast settings had to be adjusted differently for +GA (Min: 40, Max: 220) and –GA (Min: 25, Max: 100). The other parasitic structures are (E) PfNup116 (green, dilution 1:50) and (F) SBP1 (green, dilution 1:500). Contrast for Hoechst had to be adjusted differently for the respective cell in the +GA (Min: 20, Max: 180) and –GA (Min: 15, Max: 40) conditions of the anti-PfNup116 staining to allow visibility. All images except brightfield (BF) and Fig. 1B are maximum intensity projections. Scale bars, 1 µm.*

More critically, we detected, as previously found by many colleagues, a high fraction of unlabeled cells (Suppl. Fig. 2). Quantification revealed a strong drop of labeling density with GA for PbHsp70, Exp1, SBP1, and Cdc48 (apicoplast, [14], dilution 1:500) antibodies (Table 1). We did not optimize the permeabilization protocol to potentially alleviate this effect but used standard incubation conditions and Triton® X-100 concentration as described before [3]. To exclude the possibility that the lack of staining in GA-fixed cells is related to the absence of mechanical stress imposed upon cells during centrifugation, potentially improving antibody penetration, we also tested staining in suspension as described previously [3]. This approach did not improve the fraction of stained cells (Table 1). A possible explanation for the increase in labeling density under GA-free conditions may be improved penetration of the antibody to the site of binding due to partial lysis of RBCs. From our rudimentary observations we could not extract a rule predicting staining success of specific parasite stages according to hemozoin, DNA content, etc. when fixed with GA. This poses the question whether an unbiased selection of cells for quantification purposes is at all possible under these staining conditions.

Table 1. Percentage of antibody-stained cells with or without GA addition

Fixation\Antibody	anti-PbHSP70	anti-Exp1	anti-SBP1	anti-Cdc48
-GA on Lab-Tek	96.4% (187/194)	99.5% (204/205)	99.5% (189/190)	100% (132/132)
+GA on Lab-Tek	0% (0/92)	4.7% (9/191)	2.6% (3/117)	8.5% (5/59)
+GA in suspension	0% (0/62)	2.7% (2/75)	2.7% (2/73)	3.2% (2/62)

To check whether GA can occasionally prevent antibody recognition, we tested two more antibodies that had been previously unsuccessful in specifically staining *P. falciparum* blood stage parasites. We confirmed that an anti-PbHSP70 antibody [15] does not label cells with GA (Table 1) but can give a distinct cytoplasmic staining without (Fig. 2A). Further, staining with two commercial cross-species reactive anti-centrin (clone 20H5, Merck) and anti-γ-tubulin (ab16504, Abcam) antibodies revealed only background staining with GA (Fig. 2B). Under improved conditions we detected a perinuclear colocalization at a site that is presumably the centriolar plaque, thereby displaying the expected localization.

How far one can improve resolution beyond the diffraction limit is highly dependent on the number of photons that can be collected from a given sample. We therefore imaged our newly improved immunofluorescence staining samples by STED nanoscopy. An important limitation we noticed upon parasite imaging is substantial structural damage to the cells caused by the STED laser should it hit the hemozoin crystal. This can be explained by the STED laser power being about three orders of magnitude higher than standard excitation lasers and the hemozoin being a highly absorbing crystal [16]. This effect has been described before by Michael Pasternak on the STED Abberior website (www.abberior-instruments.com/products/expert-line/rescue/). Improved imaging protocols using feedback control for soft- and hardware, allowing acquisition of full iRBCs that contain hemozoin, are in principle available and need to be established in the future. As a consequence, we could only image subcellular regions devoid of hemozoin, thereby avoiding cellular damage. Based on recommendations and comparisons of

a few STED-compatible dyes, we yielded the best image quality with Atto 594-tagged secondary antibodies (anti-mouse 76085, anti-rabbit 77671, Sigma). For dual-color STED we recommend combination with Atto 647N or STAR RED fluorophores (50185, Sigma or Abberior). We chose anti-α-tubulin and anti-PfNup116 staining for microtubules and nuclear pores, respectively, to test whether we can resolve sub-diffraction structures within the parasite nucleus. Direct comparison of the same cellular region imaged in confocal and STED revealed nicely separated microtubule bundles emerging from distinct points (Fig. 2C) as well as individual nuclear pore clusters that were not distinguishable in scanning confocal images (Fig. 2D).

The amount and quality of cell biological information that can be extracted from fixed cells is highly dependent on the quality of the immunofluorescence staining. Our improvement to the state-of-the-art protocol gives an opportunity to reiterate the efficacy of previous antibodies and improve specificity for future labelling. In combination with super-resolution nanoscopy this protocol can push the boundaries of what will be discovered about sub-cellular organization in the malaria parasite a bit further.

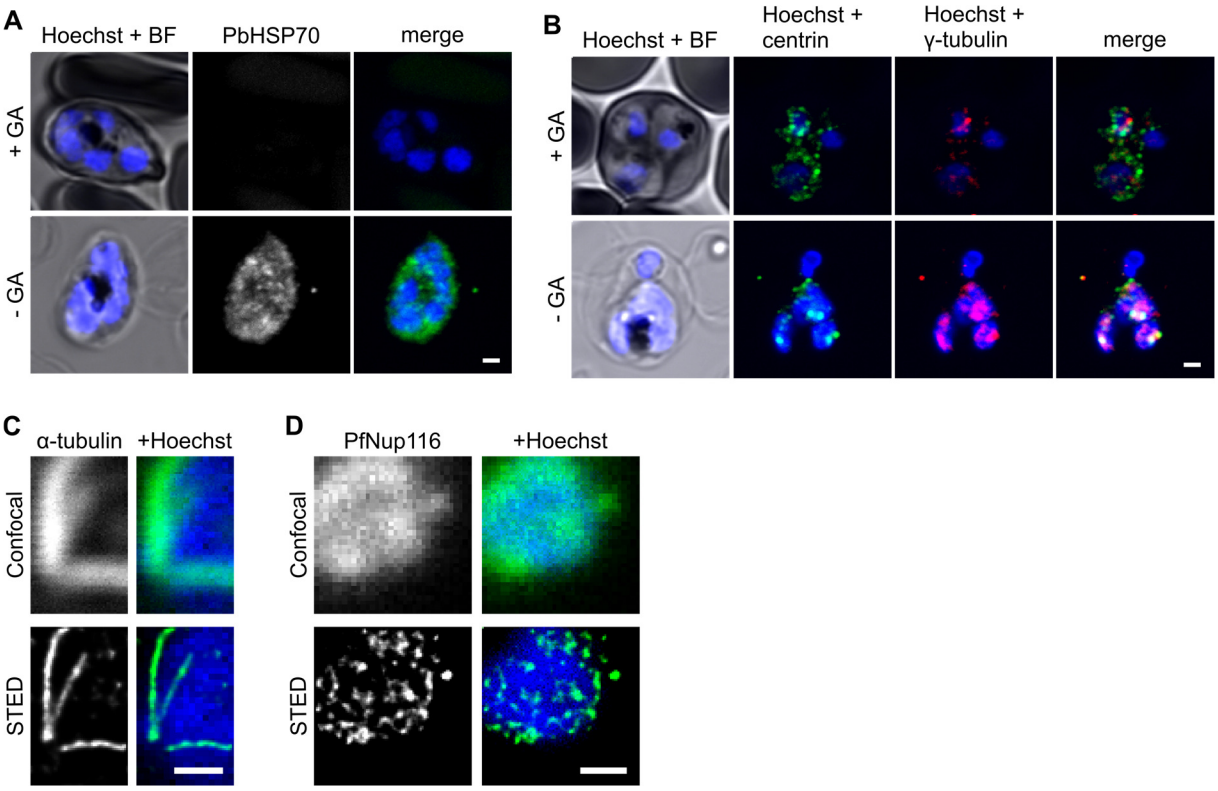

Fig. 2. Epitope masking upon fixation with GA and STED nanoscopy images of nuclear structures.
(A) Confocal images of iRBCs stained with Hoechst (blue) and labeled with anti-PbHSP70 antibody (green, dilution 1:100) after fixation with (upper panel) or without GA addition (lower panel). All images except brightfield (BF) are maximum intensity projections. Scale bar, 1 µm. (B) Co-staining of iRBCs with anti-centrin (green, dilution 1:1000) and anti-γ-tubulin antibody (red, dilution 1:100) together with Hoechst (blue). Infected RBCs were fixed with (upper panel) or without GA (lower panel). All images except brightfield (BF) are maximum intensity projections. Scale bar, 1 µm. (C) Confocal (upper panels) and deconvolved STED microscopy images (lower panels) of iRBCs, labeled by using our improved immunofluorescence protocol. Subregion of parasite labeled for microtubules by anti-α-tubulin antibody (green, dilution 1:500) and DNA by Hoechst (blue). (D) Subregion of parasite labeled for nuclear pores by anti-PfNup116 antibody (green, dilution 1:50) and DNA by Hoechst (blue). Scale bars, 500 nm.

Materials and methods

Parasite culture

P. falciparum blood stage cultures (NF54) were maintained at a hematocrit of about 3% in 37 °C incubators with 90% humidity, 5% O_2 and 3% CO_2 saturation. Culture development was monitored by Giemsa staining, and cultures were diluted with O+ human erythrocytes to maintain a parasitemia of 3–5%. Parasites were synchronized by sorbitol lysis of late stages.

Seeding infected red blood cells

Cell seeding was adapted to Lab-Tek II 8 well chambered slides (Thermo Fisher) using previously described procedure [9]. Infected RBCs containing *P. falciparum* ring stages were seeded on Lab-Tek II slides. For this purpose, Lab-Tek wells were coated with 80 µL Concanavalin A (Sigma, 5mg/ml in water) per well. After 20 min at 37 °C, wells were rinsed twice with pre-warmed PBS. For each well, 150 µL of iRBC culture was washed twice with PBS by centrifugation in 1.5 ml reaction tubes at 800 g for 15 sec and distributed into the wells. Cells were allowed to settle for 10 min at 37 °C. Unbound RBCs were carefully washed away with two to three PBS rinses until a faint RBC monolayer remained. Seeded iRBCs were incubated a few hours or overnight in 400µl complete RPMI cell culture medium, which was necessary since fixation of cells directly after iRBC seeding never allowed us to detect any spindle microtubules in the parasites (Suppl. Fig. 3). This might be due to depolymerization of these delicate structures upon osmotic stress caused by PBS or change in temperature during cell handling.

Immunofluorescence staining

Wells were quickly rinsed with PBS and immediately fixed with prewarmed 4% PFA or 4% PFA/0.0075% GA at 37 °C for 20 min. All remaining steps were performed at room temperature. After rinsing once with PBS, cells were permeabilized with 0.1% Triton® X-100 in PBS for 15 min, followed by three PBS washes. Quenching of free aldehyde groups was done in ~0.1 mg/mL $NaBH_4$ for 10 min. Cells were washed twice and blocked in 3% BSA/PBS for at least 30 min. Both primary (see figure legends for details) and secondary antibody dilutions (1:200 or 1:500) were centrifuged at 14.800 rpm for 10 min at room temperature to remove aggregates. Primary antibodies were allowed to bind for 2 h in 3% BSA/PBS followed by three washes with 0.5% Tween® 20/PBS for 5-10 min each on a horizontal shaker. Secondary antibodies and Hoechst were added in fresh blocking buffer and incubated for at least 30 min while protected from light. Cells were washed again with 0.5% Tween® 20/PBS three times and one additional time in PBS on a horizontal shaker. Samples were stored in 300 µL PBS at 4 °C in the dark until imaging. The same protocol was also applied to cells in suspension with 4% PFA/0.0075% GA fixation as described before [3]. RBC actin was stained with Phalloidin-Alexa Fluor 488 1:500 (Thermo Fisher) in PBS for 30 min.

Image acquisition and analysis

Images were acquired on a Leica TCS SP8 scanning confocal microscope, equipped with a 63x oil objective (numerical aperture, 1.4), GaAsP hybrid detectors and spectral emission filter. Laser power (405, 488, 561, 633) was individually adjusted to the different antibody combinations and fluorophores used. Images had a size of 128 x 128 pixels with a pixel size of 72 nm and pixel dwell time of 4.88 µs. Z-stacks of 4.18 µm and 6.27 µm were acquired with a step size of 280 nm. For overview images to quantify labeling efficiency we used 2048 x 2048 pixels with a pixel size of 92 nm and z-stack size of 8-10 µm. Images were merged and adjusted for contrast using Fiji [10]. Super-resolution images were acquired using a single-point scanning STED microscope by Abberior Instruments GmbH, equipped with a pulsed STED depletion laser of 775 nm, using gated detection. The STED laser power was adjusted to about 40%. Imaging was performed with a 100x oil objective (numerical aperture, 1.4) and a pixel size of 20 nm and pixel dwell time of 10 µs. Deconvolution was performed using Richardson-Lucy algorithm with default settings in IMSpector imaging software (Abberior Instruments GmbH).

Acknowledgements

Funded by the German Research Foundation (DFG) – [349355339] to JG. We thank: Ann-Kristin Mueller for providing the anti-PbHSP70 and Jude Przyborski for the anti-SBP1, anti-Cdc48 and anti-Exp1 antibodies. Jude Przyborski and Caroline Simon for critical reading of the manuscript. Vibor Laketa, Head of the Infectious Diseases Imaging Platform (www.idip-heidelberg.org), for providing microscopy access. Susann Kummer for advice on STED microscopy and sample preparation.

Conflicts of interest: none declared

References

[1] S. Eshar, N. Dahan-Pasternak, A. Weiner, R. Dzikowski, High resolution 3D perspective of Plasmodium biology: advancing into a new era., Trends Parasitol. 27 (2011) 548–554. doi:10.1016/j.pt.2011.08.002.

[2] L. Tilley, G. McFadden, A. Cowman, N. Klonis, Illuminating Plasmodium falciparum-infected red blood cells., Trends Parasitol. 23 (2007) 268–277. doi:10.1016/j.pt.2007.04.001.

[3] C.J. Tonkin, G.G. van Dooren, T.P. Spurck, N.S. Struck, R.T. Good, E. Handman, A.F. Cowman, G.I. McFadden, Localization of organellar proteins in Plasmodium falciparum using a novel set of transfection vectors and a new immunofluorescence fixation method., Mol Biochem Parasitol. 137 (2004) 13–21. doi:10.1016/j.molbiopara.2004.05.009.

[4] K.N. Richter, N.H. Revelo, K.J. Seitz, M.S. Helm, D. Sarkar, R.S. Saleeb, E. D'Este, J. Eberle, E. Wagner, C. Vogl, D.F. Lazaro, F. Richter, J. Coy-Vergara, G. Coceano, E.S. Boyden, R.R. Duncan, S.W. Hell, M.A. Lauterbach, S.E. Lehnart, T. Moser, T. Outeiro, P. Rehling, B. Schwappach, I. Testa, B. Zapiec, S.O. Rizzoli, Glyoxal as an alternative fixative to formaldehyde in immunostaining and super-resolution microscopy, EMBO J. 34 (2018) 139–159. doi:10.15252/embj.201695709.

[5] D.T. Riglar, D. Richard, D.W. Wilson, M.J. Boyle, C. Dekiwadia, L. Turnbull, F. Angrisano, D.S. Marapana, K.L. Rogers, C.B. Whitchurch, J.G. Beeson, A.F. Cowman, S.A. Ralph, J. Baum, Super-resolution dissection of coordinated events during malaria parasite invasion of the human erythrocyte, Cell Host Microbe. 9 (2011) 9–20. doi:10.1016/j.chom.2010.12.003.

[6] L. Schermelleh, P.M. Carlton, S. Haase, L. Shao, L. Winoto, P. Kner, B. Burke, M.C. Cardoso, D.A. Agard, M.G.L. Gustafsson, H. Leonhardt, J.W. Sedat, Subdiffraction multicolor imaging of the nuclear periphery with 3D structured illumination microscopy, Science. 320 (2008) 1332–1336. doi:10.1126/science.1156947.

[7] S.J. Sahl, S.W. Hell, S. Jakobs, Fluorescence nanoscopy in cell biology, Nat. Rev. Mol. Cell Biol. 18 (2017) 685–701. doi:10.1038/nrm.2017.71.

[8] C. Gruring, A. Heiber, F. Kruse, J. Ungefehr, T.W. Gilberger, T. Spielmann, Development and host cell modifications of Plasmodium falciparum blood stages in four dimensions, Nat Commun. 2 (2011) 165. doi:ncomms1169 [pii] 10.1038/ncomms1169.

[9] C. Gruring, T. Spielmann, Imaging of live malaria blood stage parasites., Methods Enzym. 506 (2012) 81–92. doi:10.1016/B978-0-12-391856-7.00029-9.

[10] J. Schindelin, I. Arganda-Carreras, E. Frise, V. Kaynig, M. Longair, T. Pietzsch, S. Preibisch, C. Rueden, S. Saalfeld, B. Schmid, J.Y. Tinevez, D.J. White, V. Hartenstein, K. Eliceiri, P. Tomancak, A. Cardona, Fiji: An open-source platform for biological-image analysis, Nat. Methods. 9 (2012) 676–682. doi:10.1038/nmeth.2019.

[11] K. Günther, M. Tümmler, H.-H. Arnold, R. Ridley, M. Goman, J.G. Scaife, K. Lingelbach, An exported protein of Plasmodium falciparum is synthesized as an integral membrane protein, Mol. Biochem. Parasitol. 46 (1991) 149–157. doi:10.1016/0166-6851(91)90208-N.

[12] T. Blisnick, M.E. Morales Betoulle, J.C. Barale, P. Uzureau, L. Berry, S. Desroses, H. Fujioka, D. Mattei, C. Braun Breton, Pfsbp1, a Maurer's cleft Plasmodium falciparum protein, is associated with the erythrocyte skeleton, Mol. Biochem. Parasitol. 111 (2000) 107–121. doi:10.1016/S0166-6851(00)00301-7.

[13] J. Guizetti, R.M. Martins, S. Guadagnini, A. Claes, A. Scherf, Nuclear pores and perinuclear expression sites of var and ribosomal DNA genes correspond to physically distinct regions in Plasmodium falciparum., Eukaryot. Cell. 12 (2013) 697–702. doi:10.1128/EC.00023-13.

[14] S. Spork, J.A. Hiss, K. Mandel, M. Sommer, T.W.A. Kooij, T. Chu, G. Schneider, U.G. Maier, J.M. Przyborski, An unusual ERAD-like complex is targeted to the apicoplast of Plasmodium falciparum, Eukaryot. Cell. 8 (2009) 1134–1145. doi:10.1128/EC.00083-09.

[15] M. Tsuji, D. Mattei, R.S. Nussenzweig, D. Eichinger, F. Zavala, Demonstration of heat-shock protein 70 in the sporozoite stage of malaria parasites, Parasitol. Res. 80 (1994) 16–21. doi:10.1007/BF00932618.

[16] Y.A. Menyaev, K.A. Carey, D.A. Nedosekin, M. Sarimollaoglu, E.I. Galanzha, J.S. Stumhofer, V.P. Zharov, Preclinical photoacoustic models: application for ultrasensitive single cell malaria diagnosis in large vein and artery, Biomed. Opt. Express. 7 (2016) 3643–3658. doi:10.1364/BOE.7.003643.